Effect of Inert Cover Gas on Performance of Radioisotope Stirling Space Power System

R. Carpenter, V. Kumar, C. Or, A. Schock

Orbital Sciences Corporation (OSC), 20301 Century Blvd., Germantown, MD 20874
(301) 428-6460, or@oscsystems.com

Abstract. This paper describes an updated Orbital design of a radioisotope Stirling power system and its predicted performance at the beginning and end of a six-year mission to the Jovian moon Europa. The design is based on General Purpose Heat Source (GPHS) modules identical to those previously developed and safety-qualified by the Department of Energy (DOE) which were successfully launched on missions to Jupiter and Saturn by the Jet Propulsion Laboratory (JPL). In each generator, the heat produced by the decay of the Pu-238 isotope is converted to electric power by two free-piston Stirling engines and linear alternators developed by Stirling Technology Company (STC), and their rejected waste heat is transported to radiators by heat pipes. The principal difference between the proposed system design and previous Orbital designs (Or et al. 2000) is the thermal insulation between the heat source and the generator's housing. Previous designs had employed multifoil insulation, whereas the design described here employs Min-K-1800 thermal insulation. Such insulation had been successfully used by Teledyne and GE in earlier RTGs (Radioisotope Thermoelectric Generators). Although Min-K is a much poorer insulator than multifoil in vacuum and requires a substantially greater thickness for equivalent performance, it offers compensating advantages. Specifically it makes it possible to adjust the generator's BOM temperatures by filling its interior volume with inert cover gas. This makes it possible to meet the generator's BOM and EOM performance goals without exceeding its allowable temperature at the beginning of the mission.

HEAT SOURCE DESIGN

The OSC generator design employs the identical GPHS modules that were successfully developed and safety-qualified by DOE for use in RTGs for JPL's missions to Jupiter (Galileo) and Saturn (Cassini). Figure 1 depicts an exploded view of such a GPHS module.

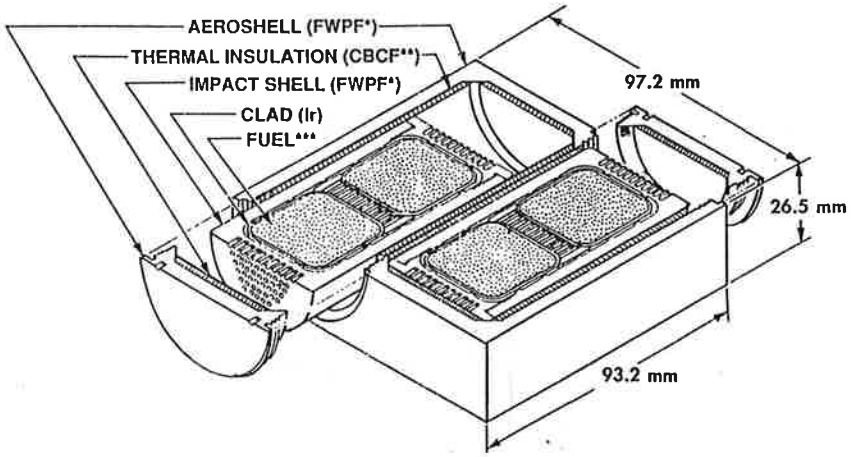

FIGURE 1. GPHS-Module (250-Watts) Sectioned at Mid-Plane.

As shown in Figure 1, each GPHS module, when freshly fueled, contains four 62.5 W(t) PuO_2 fuel pellets encapsulated in iridium-alloy clads. To prevent or minimize fuel release on Earth in normal operation and under all credible accident conditions before, during, and after launch, the fuel capsules are enclosed in graphitic safety components, consisting of an aeroshell (for ablative cooling of the module in case of inadvertent hypersonic reentry), impact shells (to protect the clads during Earth impact), and thermal insulators (to prevent overheating and retard grain growth of the iridium clads during the reentry heat pulse, and to avoid overcooling and embrittlement of the clads during the subsequent subsonic descent). The Orbital generator design uses the safety-qualified GPHS modules without any changes, to avoid the need for additional safety tests.

GENERATOR DESIGN

Figure 2 displays a 3D-cutaway view of OSC's generator design truncated at the generator's mid-plane. As shown, its radioisotope heat source, consisting of two standard GPHS modules, is located at the center of the generator, and delivers its heat output to two converters, each consisting of a free-piston Stirling engine and a linear alternator. Each engine's cold end is cooled by four low-temperature heat pipes, which deliver and distribute the generator's waste heat to a planar radiator with embedded heat pipes. The radiator also serves as the generator's mounting platform.

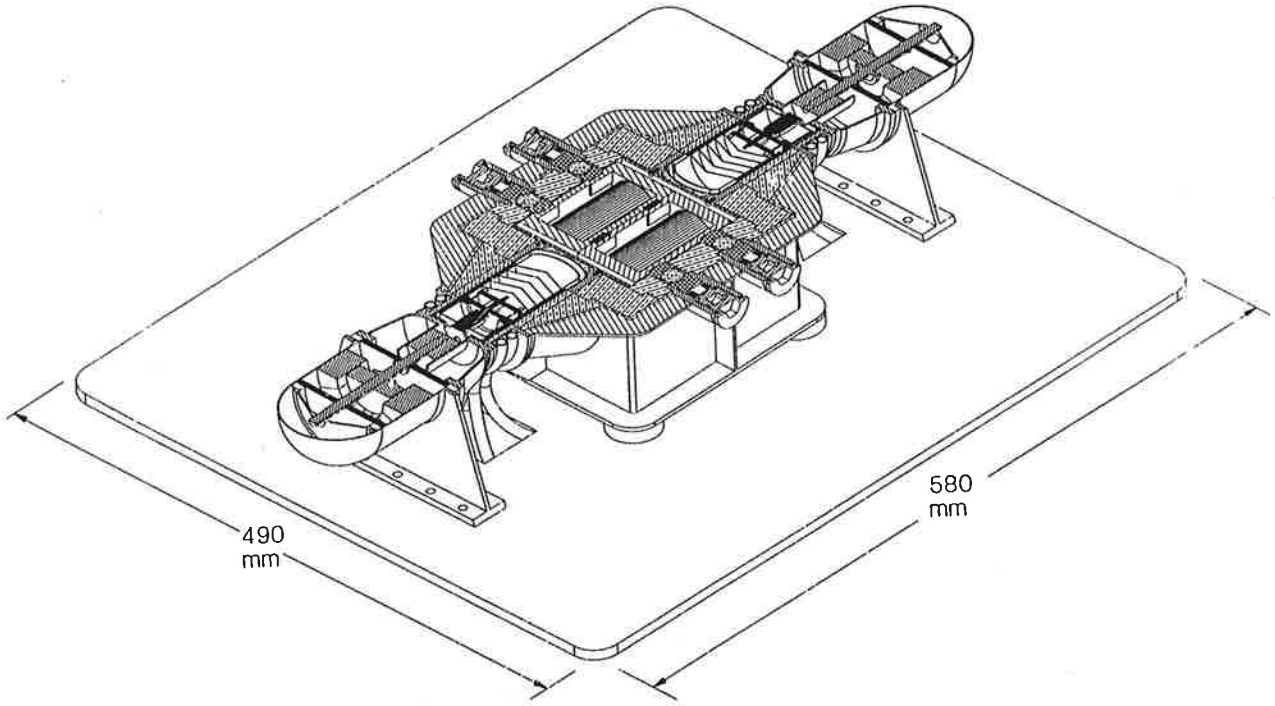

FIGURE 2. Cutaway View of OSC Generator Design.

As shown in Figure 2, each GPHS module's aeroshell contains two indentations on each of its two broadfaces. These indentations had been designed to mate with graphitic interlock buttons, which served to hold the RTG's stacked heat source modules together under transverse launch loads. The OSC Stirling generator design utilizes the same indentations to support the two GPHS modules off the generator's housing wall by means of four support subassemblies and two graphitic interlocks.

As seen, the heat source modules are insulated from the generator's housing by 1"-thick Min-K insulation. Heat transfer to the heat collectors of the two Stirling engines is by radiation across a vacuum gap and/or by conduction across an inert gas gap. There is no contact between the heat source and the two converters' heat collectors. This

minimizes structural loads on the thin engine walls due to engine vibration and thermal expansion differences. As shown, the two GPHS modules are supported from the generator's cool wall by four externally adjustable support assemblies, and from each other by two graphitic interlocks.

The heat source support subassemblies must be strong enough to resist compressive and shear loads during launch, while minimizing conductive heat losses between the hot heat source and the cool housing. As shown in Figure 3, each support subassembly contains a 15-mm diameter zirconia thermal insulator sphere in contact with hot (graphitic) and cold (metallic) cylindrical pistons. As shown, the piston seats in contact with the ZrO_2 balls are pyramid-shaped to minimize heat losses. The resultant four-point contact between pistons and balls yield lower heat losses than would a circular contact ring if pistons with conical seats were employed. The use of spherical balls enables them to provide 3-directional heat source support independent of their orientation.

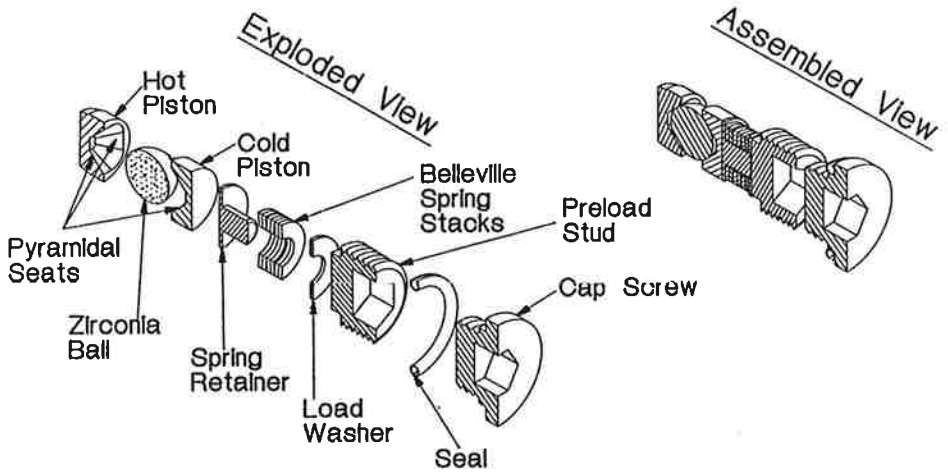

FIGURE 3. Exploded and Assembled View of Heat Source Support Subassembly.

During fueling of the heat source assembly, the support subassemblies are partially withdrawn to permit insertion of the two GPHS modules. After final assembly, the cold pistons and ZrO_2 balls are pre-loaded by nested Belleville springs compressed by threaded end caps. The compressive force exerted by the springs serves to keep the hot pistons seated in the aeroshell indentations under transverse and axial launch loads. They also serve to compress the seals between the cold pistons and the housing. The adequacy of the heat source support arrangement under typical launch loads was recently demonstrated during cold vibration tests at Mound (Davis et. al., 2000).

As shown in Figure 2, the heat produced by the radioisotope heat source is transferred to the heat collectors at the hot ends of two free-piston Stirling engines which are coupled to linear alternators. These engines and linear alternators are under development by the Stirling Technology Company. Similar STC converters have demonstrated over six years of unattended failure-free operation.

The waste heat rejected by each Stirling engine is delivered to the radiator via low-temperature heat pipes. The heat pipes are wrapped around the engines' cold ends and are embedded between the radiator's face sheets. There are four heat pipes per engine to prevent single-point failures. As shown in Figure 2, the radiator also serves as the generator's support platform.

To analyze the BOM and EOM performance of the radioisotope power system described above, OSC utilized parametric engine performance predictions supplied by Stirling Technology Company (STC). Those predictions were based on Gedeon's GLIMP code, which had previously demonstrated good agreement with experimental results. Typical STC performance predictions are shown in Table 1, for an engine design optimized (tuned) for a hot-end temperature of 650°C and a cold-end temperature of 80°C. The effects of hot- and cold-end temperatures on the engine's heat input, power output, and conversion efficiency are presented in Table 1, and are shown graphically in Figure 4. Note that the parametric performance predictions are for a fixed engine design. This is a critical point for predicting the performance of unattended Stirling power systems, which OSC found to be very sensitive to the effect of isotope decay during the mission.

TABLE 1. Effect of Hot- and Cold-End Temperatures on STC-Predicted Performance of Stirling System Optimized for 650°C and 80°C Hot- and Cold-End Temperatures.

Cold-End Temperature (C)	Hot-End Temperature (C)	Net Heat Input (W)	Net Electric Output (W)	Converter Efficiency (%)
40	400	152.4	34.9	22.9
40	450	167.4	42.5	25.4
40	500	182.5	50.0	27.4
40	550	197.2	57.4	29.1
60	400	147.9	30.8	20.8
60	450	162.7	38.2	23.5
60	500	177.5	45.5	25.6
60	550	192.3	52.8	27.4
60	600	204.2	59.5	29.1
80	400	143.5	27.0	18.8
80	450	158.5	34.1	21.5
80	500	173.0	41.3	23.9
80	550	187.3	48.4	25.8
80	600	199.5	54.9	27.5
80	650	205.8	59.7	29.0

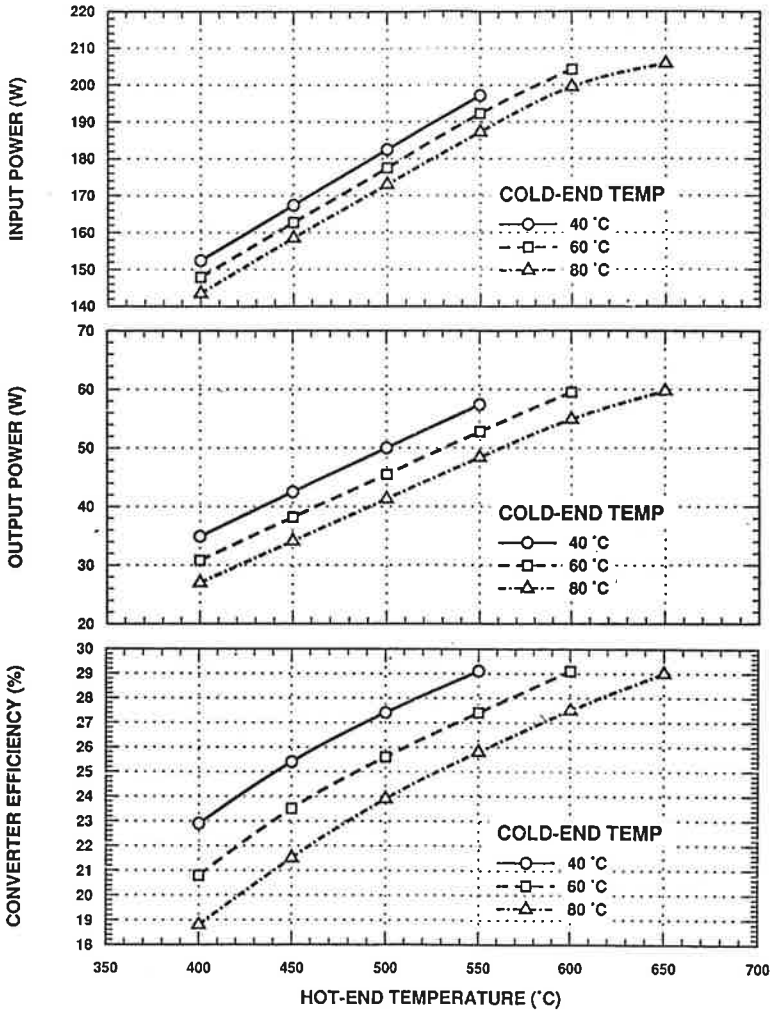

FIGURE 4. Effect of Hot- and Cold-End Temperatures on STC-Predicted Off-Optimum Performance of RG-55 Engine Design Optimized for 650°C and 80°C Temperatures.

Finally, Figure 5 illustrates a thermal model of a spacecraft with three generators. Location of the generators at the base of the spacecraft is favored by JPL spacecraft designers because it facilitates utilization of the generators' rejected waste heat for maintaining the temperatures of the spacecraft's critical components, such as fuel/oxidizer tanks and plumbing.

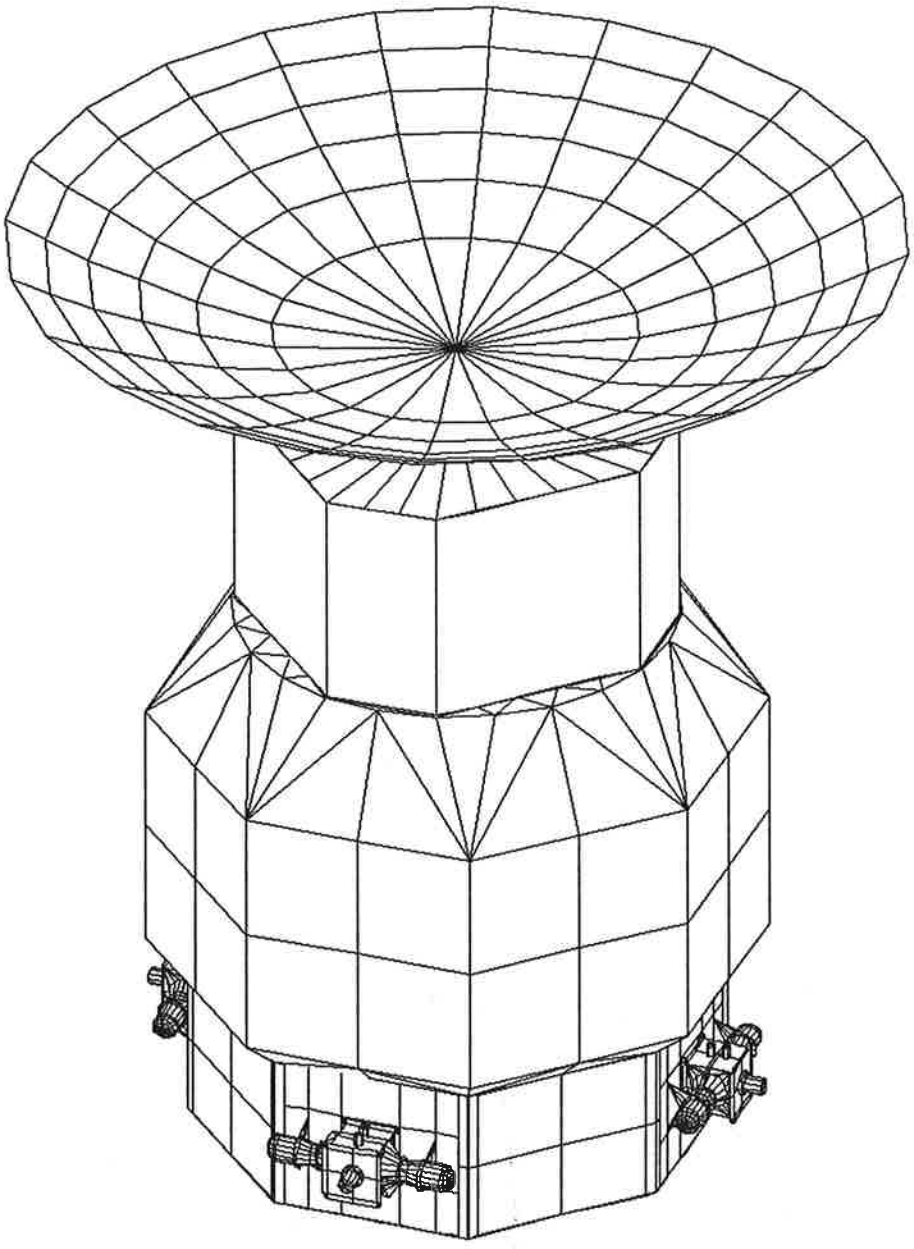

FIGURE 5. Illustrative Spacecraft Design with Three Orbital Generators.

The above-described design was modeled and analyzed by combining the SINDA (Cullimore, 1997) thermal conduction code and the SSPTA (Little, 1986) thermal radiation code with the STC-generated GLIMPS Stirling engine thermodynamic results displayed in Figure 4.

ANALYTICAL PROCEDURE

The performance of the Stirling power system was analyzed by a trial and error procedure. This procedure is illustrated in Table 2 for an evacuated power system with an EOM thermal input power of 232 W per GPHS module, and a heat collector emissivity of 0.60. The table shows the effect of the engines' hot-end temperatures on their cold-end temperatures and on the SINDA-generated net heat flow delivered to their hot ends. For each line in the table, the SINDA-generated net heat flow to the engine's hot-end is compared to the net heat flow predicted from STC's Table 1 interpolated for the same hot and cold temperatures.

Table 2. Illustrative Trial-and-Error Search for Consistent Heat Input Q to Engines.

T_{HOT} °C	T_{COLD} °C	T_R °C	Q_{SINDA} W(t)	Q_{STC} W(t)	ΔQ W_T	P_{OUT} W(DC)	η_{SYS} %
663.4	79.6	75.2	210.78	207.60	3.19	353.7	25.40
666.2	79.4	75.1	210.70	207.97	2.72	354.6	25.47
669.0	79.3	75.0	210.61	208.35	2.26	355.7	25.54
671.8	79.2	74.9	210.52	208.74	1.79	356.6	25.61
674.7	79.1	74.8	210.44	209.13	1.31	357.6	25.68
677.6	79.0	74.7	210.35	209.51	0.83	358.5	25.75
680.5	78.9	74.6	210.26	209.91	0.35	359.6	25.82
683.4	78.7	74.5	210.16	210.31	-0.14	360.6	25.89
686.4	78.6	74.4	210.07	210.70	-0.64	326.1	26.04
689.4	78.5	74.3	209.98	211.11	-1.13	362.6	26.04
692.4	78.4	74.2	209.88	211.52	-1.64	363.6	26.11

The table's left column lists a range of trial values of engine hot-end temperatures. Inserting these into the generator's SINDA model yields the cold-end and radiator temperatures shown in columns 2 and 3, and the heat input rates (Q_{SINDA}) shown in column 4. For the same hot- and cold-end temperatures, double interpolation of the STC-furnished engine performance tables shown in Table 1 and Figure 4 yields the engine heat input rates (Q_{STC}) listed in column 5 of Table 2, and the difference ΔQ between columns 4 and 5 is listed in column 6. The DC power output P_{OUT} and system efficiency η_{SYS} of the 3-generator system are shown in columns 7 and 8. The consistent solution is the line in Table 2 at which $\Delta Q=0$, which occurs at $T_{HOT}\approx 682°C$. The OSC program automatically searches for that line.

Figure 6 shows a typical solution giving the temperatures in °C of a xenon-filled generator at the end of the 6-year mission. As shown, this yields a fuel capsule clad temperature of 1168°C (which is well below the prescribed limit of 1330°C), an average GPHS aeroshell temperature of 963°C, a maximum ZrO_2 ball temperature of 713°C, and a temperature of 104°C at the heat source's aluminum housing. As shown, the temperatures of the Min-K-1800 insulator range from 91°C to 978°C, which is below its recommended 1800°F limit. The Stirling engine's maximum heat collector temperature is 772°C, and the engines' hot- and cold-side temperatures are 639°C and 81°C.

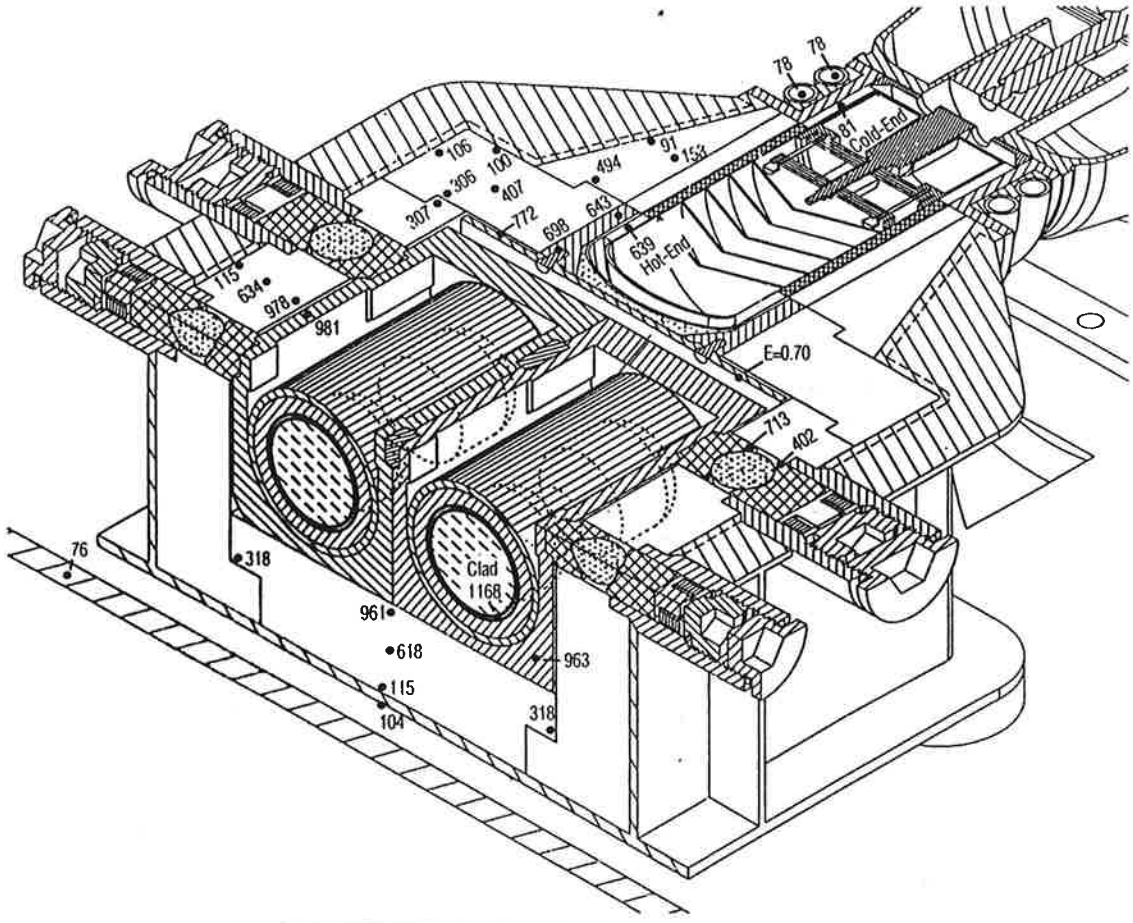

FIGURE 6. Illustrative EOM Temperatures in °C of Xenon-Filled Generator on Spacecraft.

SYSTEM ANALYSES

The OSC system analyses were carried out by the trial-and-error methodology described above. For each set of input parameters (*i.e.*, the heat source thermal power, radiator design, and heat sink parameters) the heat collector emissivity was varied and the SINDA model was used to calculate the engine's resultant hot- and cold-end temperatures and the heat input to the engine. This process was repeated iteratively until the SINDA-generated heat input matched the STC-predicted input power shown in Figure 4 interpolated for the same hot and cold temperatures. The above process was repeated for various thermal powers (ranging from 243.4 W(t) per GPHS module at BOM to 232.1 W(t) per module at EOM), for a range of heat collector emissivities (0.1 to 0.9), and for various mixtures of inert cover gases (vacuum, xenon, argon, and helium). The computed BOM and EOM results for cover gases of principal interest are summarized in Table 3, and compared with prescribed temperature limits and power goals.

The BOM results in Table 3 are for a 70% xenon and 30% helium cover gas. As shown, these yielded a 1073°C clad temperature, which is well below the 1330°C established in previous RTG programs. Similarly, the 946°C maximum insulation temperature is below the 982°C (1800°F) limit for Min-K – 1800. Also, the engine hot-end temperature matches the prescribed 650°C limit for Inconel 718, and the predicted 309 W(e) BOM system power output exceeds JPL's 260 W(e) goal at launch.

The listed EOM results are for 6 years after launch. The computed EOM results are split into two columns. The middle column is for 100% xenon and 0% helium, but that would only be possible with a highly selective vent (e.g. Viton) which favors the venting of helium over that of xenon because of the former's much smaller molecular size. If that should prove to be impractical, the alternative would be a mechanical vent to space vacuum, activated shortly before the end of mission. As shown by the right-hand column of Table 3, that would yield an evacuated generator producing 362 W(e) at EOM, which exceeds JPL's 325 W(e) EOM goal. As shown, it would meet the clad and Min-K temperature limits, but its 685°C engine hot-end temperature would exceed the 650°C limit. However, that limit is dictated by long-term creep considerations which may not be applicable if the cover gas is not vented until shortly before EOM.

This preliminary conceptual design of a Stirling generator does not yet include an emergency heat rejection sub-system which is still being defined. Such a system will probably add to the by-pass thermal losses of the generator, and could reduce the EOM hot-end temperature under vacuum operation.

TABLE 3. OSC Stirling Power System Performance Summary.

OSC POWER SYSTEM DESIGN:				
Generators per S/C		3		
GPHS Modules per Generator		2		
GPHS Modules per S/C		6		
Stirling Converters per Generator		2		
Radiators per Generator		1		
Radiator Size, cm		49 x 58		
Heat Collector Emissivity		0.70		
Generator Mass, Kg		21.3		
MISSION PHASE		BOM	EOM (6 yr)	
COVER GAS, %:				
Xenon		70	100	0
Helium		30	0	0
THERMAL INPUT, W(t):				
per GPHS Module		243.4	232.1	232.1
per Generator		486.8	464.2	464.2
per Converter		200.0	204.3	210.6
per Spacecraft		1460.4	1392.6	1392.6
TEMPERATURE, °C:	LIMIT:			
Clad	< 1330	1073	1168	1208
Min-K Insulation (max.)	< 982	946	978	945
Heat Source Housing		157	106	95
Converter Hot End	< 650	650	639	685
Converter Cold End		105	81	79
Radiator (avg.)		100	76	74
ELECTRICAL OUTPUT, W(e):				
per Converter (AC)		54.2	58.4	63.5
per Generator (DC)		103	111	121
per S/C (DC)		309	333	362
Goal (DC)		260	325	325
EFFICIENCY, %				
Thermal		82.2	88.0	90.7
Conversion (AC)		27.1	28.6	30.2
System (DC)		21.1	23.9	26.0

CONCLUSIONS

Finally, as can be seen, the fully vented evacuated system yields a higher EOM efficiency then the selectively vented unit with a xenon cover gas. Based on STC's engine performance model, the evacuated system would yield an AC conversion efficiency of 30.2% and a DC system efficiency of 26.0% at EOM, which would be over three times the efficiency of previously flown Radioisotope Thermoelectric Generators.

ACKNOWLEDGMENTS

The above-described study was supported by the Department of Energy's Office of Space and Defense Power Systems.

REFERENCES

Cullimore, Brent, SINDA/FLUINT (System Improved Numerical Differencing Analyzer and Fluid Integrator), Version CR4.0 from Cullimore and Ring Technologies, Inc., Littleton, CO, 1997.

Davis, S. Reynoso, R. Shaffer, G. Mintz, F. Norris, V. Kumar, R. Carpenter, and A. Schock, "Dynamic Test Results of a Proposed GPHS Support System and Housing for Application in an Advanced Radioisotope Power System," in proceedings of *35th Intersociety Energy Conversion Engineering Conference*, AIAA-2000-2877, 2000.

Gedeon, David. "A Globally-Implicit Stirling Cycle Simulation," American Chemical Society, 1986, pp. 550-554.

Little, A.D., SSPTA (Simplified Space Payload Thermal Analyzer), version 3.0/VAX, for the NASA/Goddard, Arthur D. Little Inc., Cambridge, MA, 1986.

Or, C., V. Kumar, R. Carpenter, and A. Schock, "Self-Supporting Radioisotope Generators with STC-55 W Stirling Converters," in proceedings of *Space Technology and Applications International Forum (STAIF- 2000)* edited by M. El-Genk, AIP Conference Proceedings 504, New York, 2000, pp. 1242-1251.